# Cronfa - Swansea University Open Access Repository

_____

This is an author produced version of a paper published in:
*Microelectronic Engineering*

_____

Cronfa URL for this paper:

_____

**Paper:**

_____

http://www.swansea.ac.uk/library/researchsupport/ris-support/

# Accepted Manuscript

## Atomic structure and band alignment at Al2O3/GaN, Sc2O3/GaN and La2O3/GaN interfaces: A first-principles study

Zhaofu Zhang, Yuzheng Guo, John Robertson

Please cite this article as: Z. Zhang, Y. Guo and J. Robertson, Atomic structure and band alignment at Al2O3/GaN, Sc2O3/GaN and La2O3/GaN interfaces: A first-principles study, Microelectronic Engineering, https://doi.org/10.1016/j.mee.2019.111039

# Atomic structure and band alignment at $Al_2O_3$/GaN, $Sc_2O_3$/GaN and $La_2O_3$/GaN interfaces: A first-principles study

Zhaofu Zhang[1], Yuzheng Guo[2], and John Robertson[1, a)]

[1]*Department of Engineering, Cambridge University, Cambridge, CB2 1PZ, United Kingdom*
[2]*College of Engineering, Swansea University, Swansea, SA1 8EN, United Kingdom*
a) *E-mail address of corresponding author:* jr214@cam.ac.uk

The atomic structures, chemical bonding and band alignment at trivalent oxides $X_2O_3$ (where X=Al, Sc and La) and GaN interface are studied based on the density functional supercell calculations. The insulating interfaces with small roughness and a clean bandgap are built based on the electron counting rule. The results prove that Ga-O bonds dominate the interfacial chemical bonding for all the interfaces, and the calculated oxide/GaN band alignment consistent with the experimental values. All the oxides are proved to have the type-I band alignment with GaN with hybrid functional calculation. For the $Al_2O_3$ interface, the calculated valence band offset is 1.17 eV, while that for the $Sc_2O_3$ and $La_2O_3$ interface are 0.81 eV and 0.95 eV, respectively. The calculated conduction band offsets are all larger than 1 eV, and as large as 1.8 eV for the $Al_2O_3$ interface. The theoretically calculated band alignments indicate that the studied trivalent oxides $Al_2O_3$, $Sc_2O_3$ and $La_2O_3$ are all suitable gate insulators for GaN-based MOSFET applications.

## 1. Introduction

Benefiting from the superior material properties such as the wide bandgap, high breakdown field, and high carrier saturation velocity, GaN semiconductor is being established as one of the most important materials for next-generation high-voltage power devices beyond silicon [1]. Compared with AlGaN/GaN high electron mobility transistor (HEMT), the GaN metal-oxide-semiconductor field-effect transistor (MOSFET) has the advantages of lower leakage current and positive threshold voltage which is more desirable for power electronics applications [2]. To maximumly enable novel functionalities and supplement the flexibility of device design in GaN-based electronics, a reliable gate insulator should be carefully selected. The trivalent oxide $Sc_2O_3$ with large bandgap ($E_g$=~6 eV), high dielectric constant ($\varepsilon$=~14), and suitable band offset (BO), has been reported to deliver low density of trap states and little leakage current at the $Sc_2O_3$/GaN interface in the past decade [3,4]. Besides, the high-$\kappa$ oxide $La_2O_3$ ($\varepsilon$=~27) has also drawn attention considering the benefit of higher dielectronic constant [5-8]. Later, the industrially preferred oxide $Al_2O_3$ became more popular taking advantages of the high breakdown electric field (~10 MV/cm), favorable band alignment with GaN, as well as an easier preparation by atomic-layer deposition (ALD) technique [9-12]. The dramatically improved device performances have been reported [13,14].

To prevent the Schottky emission of carriers and suppress the leakage current at the MOS interface, the oxide/semiconductor band offset especially the conduction band offset (CBO) should be sufficiently large (>1 eV) [15-17]. In power devices, an even larger CBO is more desirable considering the high-voltage gate driver requirement. In experiments, the interfaces of the trivalent oxides $X_2O_3$ (X=Al, Sc, and La) on GaN have all been extensively studied. Some previous work has reported the experimental BO values between GaN and oxide by x-ray photoemission spectroscopy (XPS) and/or UV photoelectron spectroscopy (UPS), while the reported valence band offsets (VBO) show a very wide difference ranging from 0.05 eV to 2.1 eV for $Al_2O_3$/GaN interface [9-12,18], and 0.4~0.8 eV for the $Sc_2O_3$ interface [19,20]. As for $La_2O_3$, the only report on $La_2O_3$/GaN claims a VBO of 0.63 eV [21]. The large uncertainty of the band alignment brings trouble for determining the quality of these gate oxide. In terms of the theoretical calculation, the accurate BOs should be derived based on the insulating interface, where no gap states emerge within the bandgap and the Fermi level lies at midgap. To achieve this goal, the electron counting rule (ECR) must always be obeyed in the interface model [22-24]. Currently, no theoretical work of the $Sc_2O_3$/GaN and $La_2O_3$/GaN interfaces have been reported, and there are only two calculations of $Al_2O_3$/GaN, but these used the crystal α-$Al_2O_3$ phase which has too large a band gap (~8.8 eV), and the significance of electron-counting was ignored [25,26]. Thus, a microscopic understanding of these $X_2O_3$/GaN

interface properties including the detailed atomic bonding and band edge line-up based on the reasonable interface configurations is highly desirable.

In this work, the atomic structures and electronic properties of the trivalent oxides $Al_2O_3$/GaN, $Sc_2O_3$/GaN and $La_2O_3$/GaN interfaces are systematically studied using first-principles calculations. To derive the band line-up with GaN, we constructed the insulating $X_2O_3$/GaN interface models for a less ionic oxide $Al_2O_3$ and two more ionic oxide $Sc_2O_3$ and $La_2O_3$. The valence band offsets are then attained using the core-level scheme [27]. Our results prove that the VBO values are 1.17 eV, 0.81 eV and 0.95 eV for $Al_2O_3$/GaN, $Sc_2O_3$/GaN and $La_2O_3$/GaN interfaces, respectively. The calculated results all fall within the range of measured data.

## 2. Methods

All the calculations were conducted using the density functional theory (DFT) plane-wave CASTEP code [28,29]. Norm-conserving pseudopotential was used, and the plane-wave cutoff energy was determined to be 700 eV. Geometry optimizations were carried out using the exchange-correlation functional of Perdew-Burke-Ernzerhof version generalized gradient approximation (GGA-PBE) [30]. A convergence criterion of 0.02 eV/Å for the force acting on each atom and a $5×5×1$ $k$-mesh was adopted. Considering the bandgap underestimation in GGA, the electronic structures were calculated by Heyd-Scuseria-Ernzerhof (HSE) hybrid functional [31] with a Hartree-Fock exchange factor of 27%, yielding the direct bandgap of 3.4 eV for wurtzite GaN bulk [32,33]. Using this HF fraction, the calculated bandgap is 6.36 eV, 5.25 and 5.65 eV for $Al_2O_3$, $Sc_2O_3$ and $La_2O_3$, respectively. The bandgap of $La_2O_3$ is almost the same with the experimental one (5.5 eV [21]), but bandgap values for $Al_2O_3$ and $Sc_2O_3$ are still 0.2 eV and 0.7 eV smaller than that of the experimental counterparts. With a larger HF fraction, the correct bandgap of oxide can be obtained, but the GaN counterpart will be otherwise overestimated. In our work, the focus is the GaN side, and the little underestimation of oxide's bandgap (< 0.7 eV) is acceptable compare with the experiment data (~6 eV). The final relaxed bulk structures are depicted in Fig. 1 and the calculated total density of states (DOS) are shown in Fig. 2.
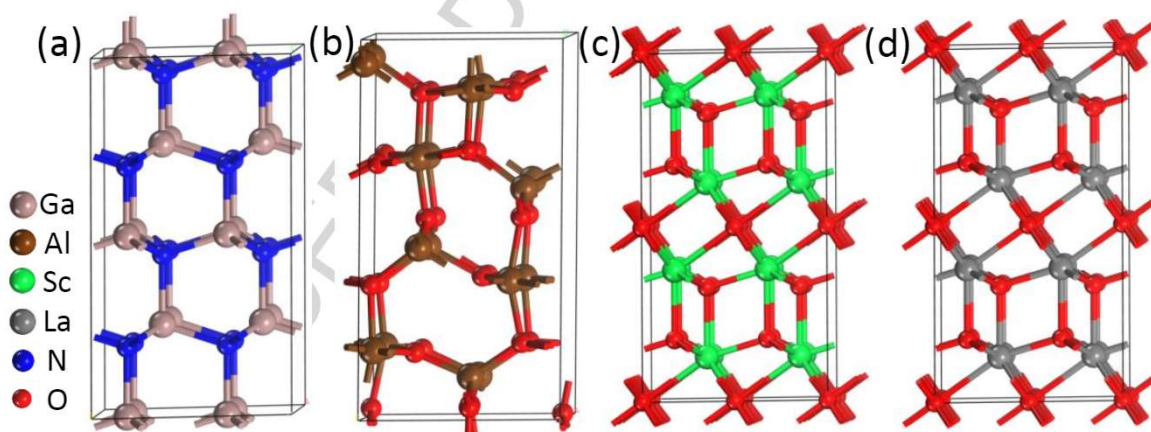


**Fig. 1.** The optimized atomic structures of (a) GaN, (b) $Al_2O_3$, (c) $Sc_2O_3$ and (d) $La_2O_3$ bulk, respectively. The species of atoms are indicated in the insert.
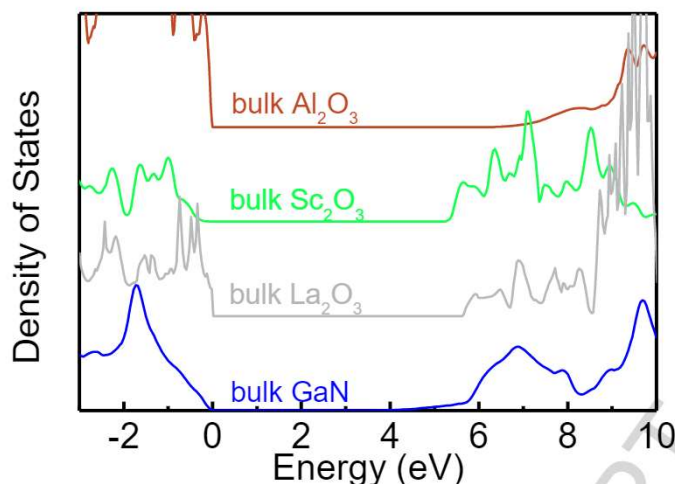
**Fig. 2.** DOS of bulk $Al_2O_3$, $Sc_2O_3$, $La_2O_3$ and GaN with HSE hybrid functional calculation. Note that CBM of GaN bulk is too weak and the bandgap is obtained from the Gamma point data.

It is noted that despite that the deposited oxide materials normally feature the amorphous phase, the essential requirement for interface modeling is the atomic local bonding rather than long-range crystalline symmetry. Realistic $Al_2O_3$ has several symmetric crystalline phases, among which the most stable one is the hexagonal $\alpha$-$Al_2O_3$ phase (i.e., corundum, or sapphire) [34], but the mass density (~4.0 $gm/cm^3$) and bandgap (~8.8 eV) in $\alpha$-$Al_2O_3$ is too high compared to the amorphous $Al_2O_3$. In the previous computational reports on $Al_2O_3$/GaN interfaces, the $\alpha$-$Al_2O_3$ were adopted, benefiting from a smaller lattice mismatch with wurtzite GaN [25,26]. As a result, the results may vary from the realistic interface configurations and thus the properties. Therefore, we adopted a modified $\theta$-phase $Al_2O_3$ structure which has a mass density (~3.5 $g/cm^3$), bandgap (~6.6 eV) and atomic coordination similar to the amorphous structure grown by ALD [34,35]. To build the interface model, the $\theta$-phase $Al_2O_3$ was strained to an orthorhombic structure and stretched laterally to match GaN (0001) surface slab, before being fully relaxed to release the internal stress. The atomic configuration for this modified $Al_2O_3$ is shown in Fig. 1(b), similar to our previous structure [35]. For the ionic oxide $Sc_2O_3$ and $La_2O_3$, the hexagonal phase was adopted, as shown in Fig. 1(c) and (d). In the supercell slab, a 15 Å thickness vacuum was added on top of the oxide. The bottom N atomic layer in GaN was passivated. Half of the top O atoms were removed to generate an insulating oxide surface without gap states.

We built the interface supercell model of (2×4) in-plane periodicity to guarantee a closed-shell structure. The supercell contains the GaN (0001) slab and the oxide surface slab with Ga-O bonding at the interface. The interface with Ga-O bonding is more favorable than other interfaces that with X-Ga or X-N interfacial bonding, because trivalent Ga is the same group with Al to make sure the local bonding of interfacial atoms resemble that in the bulk materials. Furthermore, Chokawa et al. have reported the Ga-Al interface shows amounts of interfacial defect states compared with the Ga-O model [26]. In this (2×4) interface, eight Ga and eight O atoms initially lie at the interface. For the covalent oxide $Al_2O_3$, the interfacial oxygen atoms perfectly saturate the Ga dangling bonds (DBs). While for the ionic oxide $Sc_2O_3$ and $La_2O_3$, both fourfold and sixfold O atoms exist in different layers within their bulk materials. The interfacial eight Ga DBs tend to lose six electrons in total, which should be perfectly obtained by the O DBs. As a result, only four fourfold interfacial O atoms are required so that all the O DBs are occupied according to the electron counting rule. Thus, we built the $Sc_2O_3$/GaN and $La_2O_3$/GaN interface models with only 50% interface O content (four fourfold interfacial O atoms).

## 3. Results

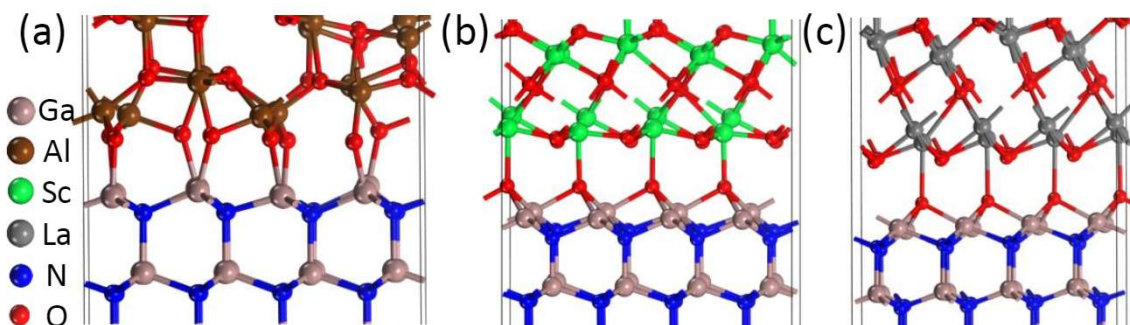**Fig. 3.** The atomic structures of final relaxed (a) $Al_2O_3$/GaN, (b) $Sc_2O_3$/GaN and (c) $La_2O_3$/GaN interfaces.

In the final relaxed $Al_2O_3$/GaN interface model shown in Fig. 3(a), the atomic structure in $Al_2O_3$ side varies from that in the crystalline phase, but the local bonding and atomic coordination remain the same. The interface is stable with a negligible roughness of only 0.3 Å at the interfacial Ga atom layer. In Fig. 3(a), the interfacial O atoms are either twofold or threefold, the same as its bulk bonding characteristics. Eight Ga-O bonds occur at the interface and each Ga atom occupies one Ga-O bond. As a result, the Ga DBs are perfectly saturated and thus an insulating interface. The average interfacial Ga-O bond length is 1.91 Å, indicating the stable covalent bonding. For the ionic oxide $Sc_2O_3$ ($La_2O_3$) interface in Fig. 3(b) (Fig. 3(c)), there are eight Ga atoms and four fourfold O atoms at the interface to satisfy the electron counting rule. These interfacial O atoms bond to one Sc (La) atom on top and three Ga atoms underneath, the same as its bulk bonding characteristics. The interface roughness is 0.29 Å (0.3 Å) with an average Ga-O bond length of 2.08 Å (2.07 Å), like that in the bulk β-$Ga_2O_3$. The interfacial Ga-O interaction barely affects the local bonding of the X (Al, Sc and La) atoms in oxide side and N atoms in GaN side, indicating the energy-stable $X_2O_3$/GaN interface configurations.
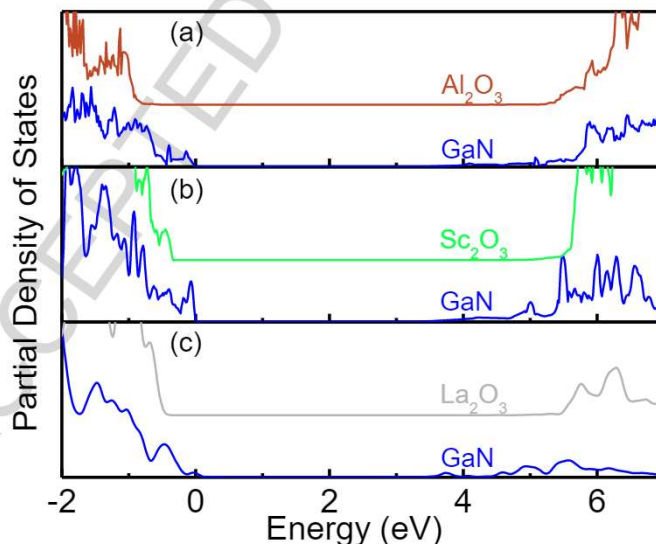


**Fig. 4.** Partial DOS of the bulk GaN and oxide atoms that lie far away from the interface region in the (a) $Al_2O_3$/GaN, (b) $Sc_2O_3$/GaN and (c) $La_2O_3$/GaN models. VBM of GaN bulk is referred to 0 eV.

Fig. 4 presents the partial density of states (PDOS) of the bulk region GaN and oxide atoms that are far away from the interface region in $X_2O_3$/GaN supercell. The valence band maximum (VBM) of GaN PDOS is aligned to zero for convenience. It is obvious that the three prudently built models all have an insulating interface without any gap states in the bandgap, benefiting from the perfect satisfaction of the electron-counting rule. The VBM and CBM at the oxide side straddle the GaN

side, i.e., the type-I band alignment. This is consistent with the electron affinity and results by the charge neutrality level (CNL) model [17,36], as well as the experiment results (see Table 1).

When semiconductor and insulator contact, discontinuous offsets (i.e., band offsets) occur at both the VBM and conduction band minimum (CBM) [15,16]. The PDOS scheme can be used to roughly determine the band edge line-up in the interface supercell model [37,38]. Using this method, the energy difference between their valence band maxima (i.e., VBO) is roughly observed to be 0.9 eV, 0.4 eV and 0.5 eV for $Al_2O_3$/GaN, $Sc_2O_3$/GaN and $La_2O_3$/GaN in Fig. 4, respectively. The counterpart CBOs can be derived as the energy difference between the calculated the band gaps values (3.4 eV, 6.36 eV, 5.25 eV and 5.65 eV for GaN and $X_2O_3$, respectively) and VBOs. In this work, we focus on another more accurate scheme to determine the band edge line-up using the core-level state [27], for the assumption that the energy difference between the VBM and the core-level state maintains a constant value in either bulk or interface environment. We used the Ga-$3d$ and O-$2s$ core-level state of atoms in the bulk-like region which are unaffected by the interface interaction, and derived the VBM of the individual side in the interface model with respect to this, and thus the VBO as the difference.
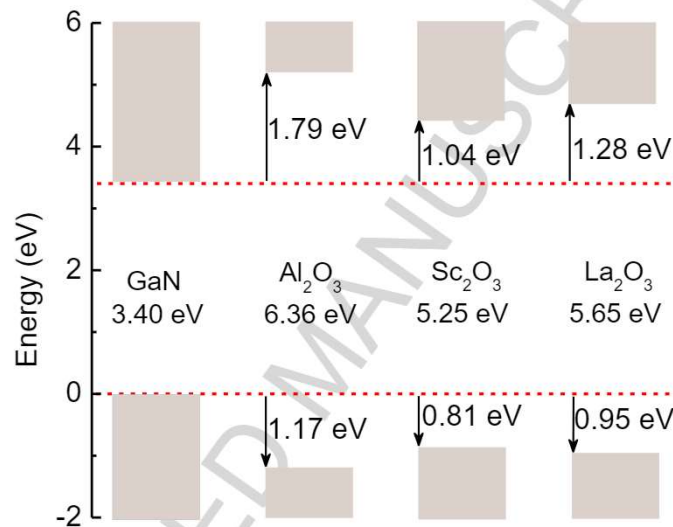


**Fig. 5.** Schematic band alignment diagram of $Al_2O_3$/GaN, $Sc_2O_3$/GaN and $La_2O_3$/GaN interfaces. The VBOs are determined using the core-level alignment scheme, which provides more accuracy. The CBOs are defined as the energy difference between the calculated bandgap and VBO values.

Fig. 5 shows the schematic band alignment diagram of $X_2O_3$/GaN interface using the core-level alignment method. It is worth noting that the calculated bandgap for $Al_2O_3$ and $Sc_2O_3$ are 6.36 eV and 5.25 eV, respectively, which are still 0.2 eV and 0.7 eV lower than that of the experimental data [9,19]. The results presented here can still be appreciated because the experimental bandgap value of GaN ($E_g$=3.4 eV) is well reproduced. Besides, the bandgap of $La_2O_3$ is similar to the experimental one [21]. The calculated VBO is 1.17 eV, 0.81 eV, and 0.95 eV for $Al_2O_3$/GaN, $Sc_2O_3$/GaN and $La_2O_3$/GaN, respectively. Taking advantage of the calculated oxide bandgap, the corresponding CBO is set to be 1.79 eV, 1.04 eV and 1.28 eV, respectively. Here the similarity of VBOs in $Sc_2O_3$/GaN and $La_2O_3$/GaN is owing to the VBMs to of the two oxides are both nonbonding O-$2p$ states and so they lie at similar energy, so that the oxide bandgap narrows by lowering CBM edge with little shift of the VBM. This agrees with our previous work on $GeO_2$ and $SiO_2$ [37], and the VBO trend coinciding with the results by CNL model in Ref. [17,36].

**Table 1** Calculated band alignment at $X_2O_3$/GaN interface, compared to the experimental reports. Note that the bandgap and BOs described in this work are all obtained by hybrid functional calculations.

| $E_g$ of $Al_2O_3$ (eV) | $E_g$ of GaN (eV) | VBO (eV) | CBO (eV) | Data |
|---|---|---|---|---|
| 6.36 | 3.40 | 1.17 | 1.79 | This work |
| 6.7 | 3.4 | 2.1 | 1.2 | Ref. [9] |
| 6.5 | 3.4 | 1.8 | 1.3 | Ref. [10] |
| 6.6 | 3.4 | 1.0 | 2.2 | Ref. [11] |
| - | - | 0.7 | - | Ref. [12] |
| 6.4 | 3.4 | 0.05 | 2.95 | Ref. [18] |
| $E_g$ of $Sc_2O_3$ (eV) | $E_g$ of GaN (eV) | VBO (eV) | CBO (eV) | Data |
| 5.25 | 3.40 | 0.81 | 1.04 | This work |
| 6.00 | 3.44 | 0.42 | 2.14 | Ref. [19] |
| 6.30 | 3.42 | 0.84 | 2.04 | Ref. [20] |
| $E_g$ of $La_2O_3$ (eV) | $E_g$ of GaN (eV) | VBO (eV) | CBO (eV) | Data |
| 5.65 | 3.40 | 0.95 | 1.28 | This work |
| 5.50 | 3.40 | 0.63 | 1.47 | Ref. [21] |
| 5.70 | 3.42 | 0.88 | 1.40 | Ref. [39]* |

*Ref. [39] measured the lanthanum silicate $(La_2O_3)_{0.5}(SiO_2)_{0.5}$/GaN interface.

It is of importance to compare our calculated band alignment with the experimental values. All the experimental reported band offsets of $X_2O_3$/GaN are listed in Table 1, with the calculated data (this work) for comparison. Apparently, the calculated VBOs all fall within the experiment range. At variance with the experimental derived CBOs, the calculated CBOs are lower than several references for $Al_2O_3$ and $Sc_2O_3$ interfaces. It is because the $Al_2O_3$ and $Sc_2O_3$ bandgaps are still underestimated (0.2 eV and 0.7 eV lower than that of the experimental data, respectively [9,19]).

If taking advantage of the experimental bandgap (~6.6 eV for $Al_2O_3$ and ~6.0 for $Sc_2O_3$ [9,19]) and our calculated VBOs, the newly derived CBO will be ~2.0 eV for $Al_2O_3$ interface and ~1.8 for $Sc_2O_3$ interface, which agrees better with the experimental CBO values. As for $La_2O_3$, our VBO (0.95 eV) is a little larger than the only experiment report of 0.63 eV [21], but close to that measured on the lanthanum silicate $(La_2O_3)_{0.5}(SiO_2)_{0.5}$/GaN interface [39].

Notably, the CBM at GaN side is >1 eV lower than that of $X_2O_3$ (even 1.8 eV for $Al_2O_3$/GaN), well satisfying the 1 eV criterion for confining electrons at semiconductor side [15,36]. In GaN-based power device applications, the gate electrode could suffer a large gate voltage to drive the power module. With the sufficiently large CBOs, the electrons can be effectively confined in the GaN side, further confirming that the studied trivalent oxides are suitable dielectric materials for GaN-based MOSFET device applications in terms of the band edge line-up.

## 4. Conclusions

In conclusion, to evaluate the quality of the trivalent oxides $Al_2O_3$, $Sc_2O_3$ and $La_2O_3$ as the gate insulator for GaN-based power devices, the interfacial chemical bonding and electronic structures at $X_2O_3$/GaN interface were intensively investigated. By interface modeling based on electron counting rule, the insulating interface model with clean bandgap was built. The valence band offset is calculated to be ~1.2, ~0.8 eV and ~0.9 eV, respectively, well agreeing with the experiment reports. The large conduction band offset (>1 eV) is sufficient for effectively confining electrons in GaN-based MOSFET device with these trivalent oxides as gate dielectric and $Al_2O_3$ stands out with a 1.8 eV CBO.

# References

[1] J.Y. Tsao, S. Chowdhury, M.A. Hollis, D. Jena, N.M. Johnson, K.A. Jones, R.J. Kaplar, S. Rajan, C.G. Van de Walle, E. Bellotti, C.L. Chua, R. Collazo, M.E. Coltrin, J.A. Cooper, K.R. Evans, S. Graham, T.A. Grotjohn, E.R. Heller, M. Higashiwaki, M.S. Islam, P.W. Juodawlkis, M.A. Khan, A.D. Koehler, J.H. Leach, U.K. Mishra, R.J. Nemanich, R.C.N. Pilawa-Podgurski, J.B. Shealy, Z. Sitar, M.J. Tadjer, A.F. Witulski, M. Wraback, J.A. Simmons, Adv. Electron. Mater. 4 (2018) 1600501.

[2] K.J. Chen, O. Häberlen, A. Lidow, C.L. Tsai, T. Ueda, Y. Uemoto, Y. Wu, IEEE Trans. Electron Devices 64 (2017) 779.

[3] R. Mehandru, B. Luo, J. Kim, F. Ren, B.P. Gila, A.H. Onstine, C.R. Abernathy, S.J. Pearton, D. Gotthold, R. Birkhahn, B. Peres, R. Fitch, J. Gillespie, T. Jenkins, J. Sewell, D. Via, A. Crespo, Appl. Phys. Lett. 82 (2003) 2530.

[4] X. Wang, O.I. Saadat, B. Xi, X. Lou, R.J. Molnar, T. Palacios, R.G. Gordon, Appl. Phys. Lett. 101 (2012) 232109.

[5] S.Y. No, D. Eom, C.S. Hwang, H.J. Kim, J. Appl. Phys. 100 (2006) 024111.

[6] H. Chiu, C. Lin, C. Chen, C. Yang, C. Lin, J.S. Fu, L. Chang, R. Lin, K. Hsueh, J. Electrochem. Soc. 157 (2010) H160.

[7] C.Y. Tsai, T.L. Wu, A. Chin, IEEE Electron Device Lett. 33 (2012) 35.

[8] J. Chen, T. Kawanago, H. Wakabayashi, K. Tsutsui, H. Iwai, D. Nohata, H. Nohira, K. Kakushima, Microelectron. Reliab. 60 (2016) 16.

[9] J. Yang, B.S. Eller, R.J. Nemanich, J. Appl. Phys. 116 (2014) 123702.

[10] J. Yang, B.S. Eller, C. Zhu, C. England, R.J. Nemanich, J. Appl. Phys. 112 (2012) 053710.

[11] Y. Jia, J.S. Wallace, E. Echeverria, J.A. Gardella, U. Singisetti, Phys. Status Solidi B 254 (2017) 1600681.

[12] T.L. Duan, J.S. Pan, D.S. Ang, Appl. Phys. Lett. 102 (2013) 201604.

[13] S. Yang, Z. Tang, K. Wong, Y. Lin, C. Liu, Y. Lu, S. Huang, K.J. Chen, IEEE Electron Device Lett. 34 (2013) 1497.

[14] D.M. Zhernokletov, M.A. Negara, R.D. Long, S. Aloni, D. Nordlund, P.C. McIntyre, ACS Appl. Mater. Interfaces 7 (2015) 12774.

[15] J. Robertson, J. Vac. Sci. Technol. B 18 (2000) 1785.

[16] Y. Guo, H. Li, S.J. Clark, J. Robertson, J. Phys. Chem. C 123 (2019) 5562.

[17] J. Robertson, B. Falabretti, J. Appl. Phys. 100 (2006) 014111.

[18] M.R. Coan, J.H. Woo, D. Johnson, I.R. Gatabi, H.R. Harris, J. Appl. Phys. 112 (2012) 024508.

[19] J.J. Chen, B.P. Gila, M. Hlad, A. Gerger, F. Ren, C.R. Abernathy, S.J. Pearton, Appl. Phys. Lett. 88 (2006) 142115.

[20] C. Liu, E.F. Chor, L.S. Tan, Y. Dong, Phys. Status Solidi C 4 (2007) 2330.

[21] J.F. Ihlefeld, M. Brumbach, S. Atcitty, Appl. Phys. Lett. 102 (2013) 162903.

[22] M.D. Pashley, Phys. Rev. B 40 (1989) 10481.

[23] L. Lin, J. Robertson, Appl. Phys. Lett. 98 (2011) 082903.

[24] L. Lin, Y. Guo, R. Gillen, J. Robertson, J. Appl. Phys. 113 (2013) 134103.

[25] M.B. Pereira, E.M. Diniz, S. Guerini, Adv. Cond. Matter Phys. 2015 (2015) 1.

[26] K. Chokawa, E. Kojima, M. Araidai, K. Shiraishi, Phys. Status Solidi B. 255 (2018) 1700323.

[27] E.A. Kraut, R.W. Grant, J.R. Waldrop, S.P. Kowalczyk, Phys. Rev. Lett. 44 (1980) 1620.

[28] S.J. Clark, M.D. Segall, C.J. Pickard, P.J. Hasnip, M.J. Probert, K. Refson, M.C. Payne, Z. Kristallogr. 220 (2005) 567.

[29] S.J. Clark, J. Robertson, Phys. Rev. B 82 (2010) 85208.

[30] J.P. Perdew, K. Burke, M. Ernzerhof, Phys. Rev. Lett. 77 (1996) 3865.

[31] J. Heyd, G.E. Scuseria, M. Ernzerhof, J. Chem. Phys. 124 (2006) 219906.

[32] Z. Zhang, B. Li, Q. Qian, X. Tang, M. Hua, B. Huang, K.J. Chen, IEEE Trans. Electron Devices 64 (2017) 4036.

[33] Z. Zhang, Q. Qian, B. Li, K.J. Chen, ACS Appl. Mater. Interfaces 10 (2018) 17419.

[34] D. Liu, S.J. Clark, J. Robertson, Appl. Phys. Lett. 96 (2010) 032905.

[35] D. Liu, J. Robertson, Microelectron. Eng. 86 (2009) 1668.

[36] J. Robertson, J. Vac. Sci. Technol. A 31 (2013) 50821.

[37] L. Lin, K. Xiong, J. Robertson, Appl. Phys. Lett. 97 (2010) 242902.

[38] Z. Zhang, R. Cao, C. Wang, H. Li, H. Dong, W. Wang, F. Lu, Y. Cheng, X. Xie, H. Liu, K. Cho, R. Wallace, W. Wang, ACS Appl. Mater. Interfaces 7 (2015) 5141.

[39] L.G. Gao, B. Xu, H.X. Guo, Y.D. Xia, J. Yin, Z.G. Liu, Appl. Phys. Lett. 94 (2009) 252901.
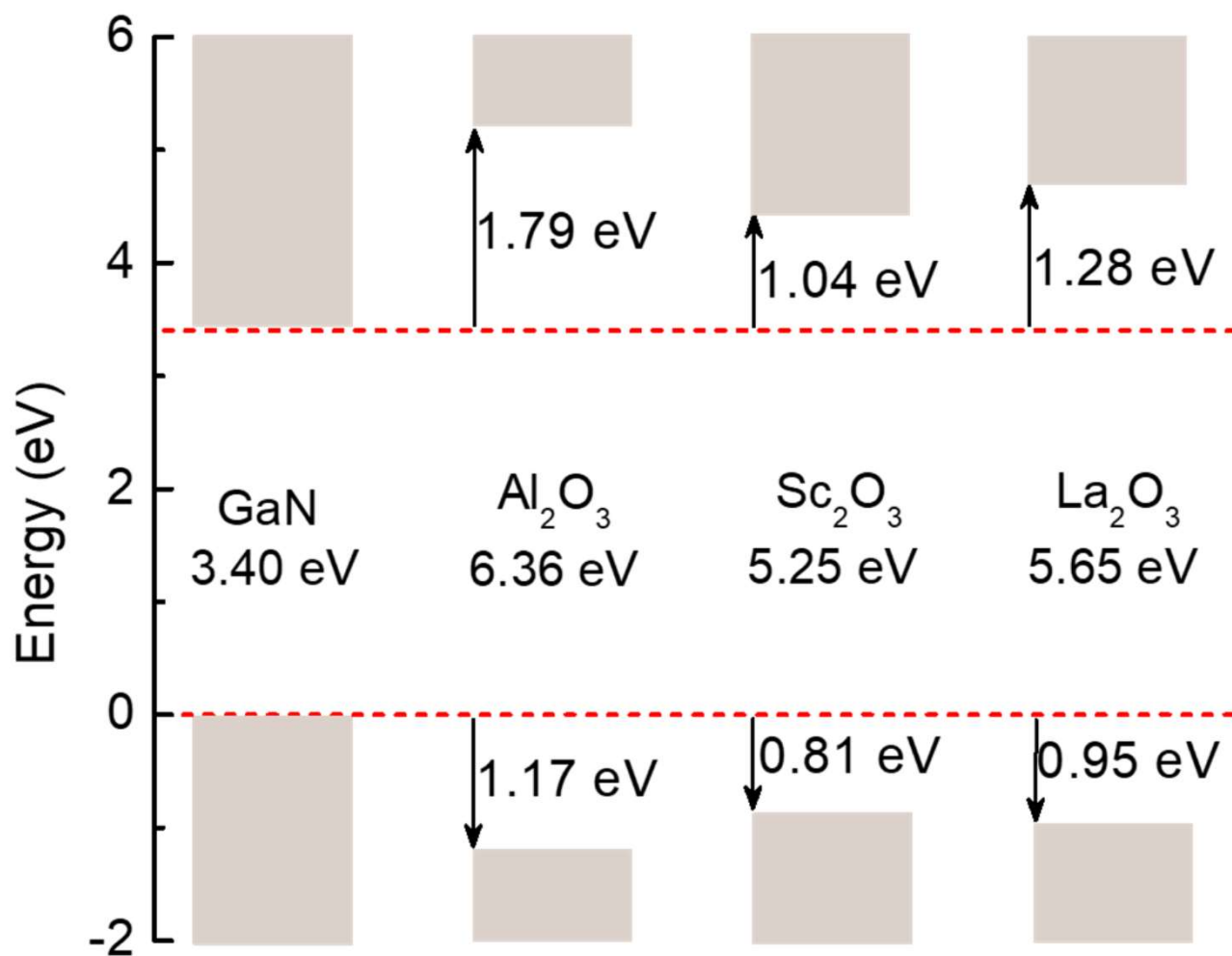
Graphical abstract

Research Highlights:
- The insulating $X_2O_3$/GaN interfaces are built based on the electron counting rule.
- Ga-O bonds dominate the interfacial chemical bonding.
- The three oxides are suitable gate insulators for GaN MOSFET in terms of band alignment.